

Polymer Chemistry

Accepted Manuscript



This is an *Accepted Manuscript*, which has been through the Royal Society of Chemistry peer review process and has been accepted for publication.

Accepted Manuscripts are published online shortly after acceptance, before technical editing, formatting and proof reading. Using this free service, authors can make their results available to the community, in citable form, before we publish the edited article. We will replace this *Accepted Manuscript* with the edited and formatted *Advance Article* as soon as it is available.

You can find more information about *Accepted Manuscripts* in the [Information for Authors](#).

Please note that technical editing may introduce minor changes to the text and/or graphics, which may alter content. The journal's standard [Terms & Conditions](#) and the [Ethical guidelines](#) still apply. In no event shall the Royal Society of Chemistry be held responsible for any errors or omissions in this *Accepted Manuscript* or any consequences arising from the use of any information it contains.

Cite this: DOI: 10.1039/c0xx00000x

www.rsc.org/xxxxxx

ARTICLE TYPE

Synthesis and Investigation of a Erbium-Containing Photosensitive Polymer

Dongfeng Fan^{1,2}, Xu Fei^{1*}, Jing Tian³, Longquan Xu¹, Xiuying Wang¹, Shuqi Fan², Yi Wang³

Received (in XXX, XXX) Xth XXXXXXXXX 20XX, Accepted Xth XXXXXXXXX 20XX

DOI: 10.1039/b000000x

Abstract

Er organic complexes are generally used in polymer-based optical amplifiers by doping. This study presents a method for creating an Er-containing photosensitive polymer by free radical copolymerization. Two types of Er organic complexes containing polymeric reactivity groups are synthesized and investigated. Er(TTA)₂(Phen)(MA), which has high photoluminescence, was polymerized with glycidyl methacrylate (GMA) for use as a novel UV-written polymer material. Poly (GMA-co-Er(TTA)₂(Phen)(MA)) were prepared with different proportions of Er, and their spectroscopic properties were investigated in detail. Polymer films with the optimum proportion (the molar ratio of GMA and Er(TTA)₂(Phen)(MA) was 115:1) exhibited good UV-light lithograph sensitivity, narrow near-infrared luminescence, good thermal stability (T_d: up to 303 °C), and solvent resistance after crosslinking. Micro patterns with smooth top surfaces were fabricated from the resulting polymer by direct UV exposure and chemical development.

1. Introduction

Optical waveguide amplifiers play a key role in optical signal transmission and manipulation because all components in a real telecommunications system suffer from losses^{1, 2}. A growing demand exists for low-cost near-infrared (NIR) light sources for communications³⁻⁵. In recent years, Er-doped waveguide amplifiers (EDWAs) have aroused significant research attention in the field of telecommunications because the infrared emission properties of Er³⁺ ion at around 1530 nm is suitable for long distance communications⁶⁻¹⁰. The two main issues faced by current amplifiers, which rely on Er ions in a glass matrix, are the difficulty of integrating onto a single substrate and the need for high pump power densities to produce gain¹.

The use of polymeric hosts for the fabrication of optical waveguide amplifiers offers many advantages, including low fabrication costs, simplified processing steps, and compatibility with processing techniques for patterning¹¹⁻¹⁴. Reports on the fabrication of organic EDWAs are numerous. One application of Er complexes is Er-doped polymers, which possess the advantages of Er complexes and the polymer matrix¹⁵⁻¹⁷. Despite the obvious advantages of such physical blending-type polymers, complexes are difficult to disperse in polymers, thus usually leading to phase separation¹⁸. Few successful polymer-based EDWAs have been demonstrated to date.

This problem can largely influence the luminescence of Er-doped polymers. Thus, we attempt to introduce an organic ligand (methacrylic acid) with excellent polymerization activity that can provide carboxyl groups as coordinating groups for Er³⁺. In

general, methacrylic acid plays a dual role as an organic ligand and compatilizer; thus, Er chelates can use olefinic double bonds to copolymerize with other monomers. At the same time, direct-write UV lithography in cationically polymerized epoxy resins is one of the most promising technologies for fabricating patterns, such as nanoscale structures¹⁹⁻²⁴. The photo-writing process of the channel waveguides into a polymer film has the advantage of a few numbers of steps and will enable us to consider the advantageous connecting operations and vertical integrated functions.

In this paper, the Er organic complexes of Er(DBM)₂(Phen)(MA) and Er(TTA)₂(Phen)(MA) were synthesized and their photoluminescence properties were investigated. The complex Er(TTA)₂(Phen)(MA) was polymerized with glycidyl methacrylate (GMA). Thereafter, transparent polymer films were formed by coating the crosslinkable copolymers (Poly (GMA-co-Er(TTA)₂(Phen)(MA))) with diphenyliodonium hexafluorophosphate as a photo initiator (PI) onto a substrate. After exposure to UV light (365 nm), the polymer formed a matrix of highly crosslinked structure. The polymer also exhibited efficient NIR emission, good chemical resistance, and excellent processability.

2. Experimental Section

2.1 Materials

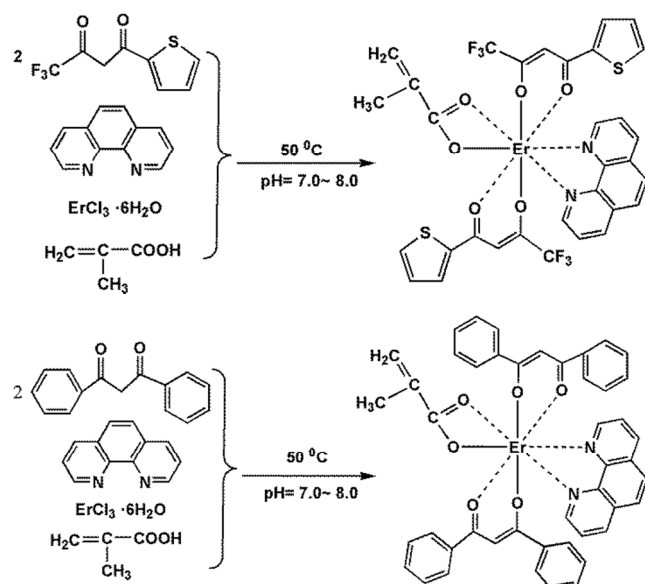
2-Thenoyltrifluoroacetone (TTA), 1,10-Phenanthroline monohydrate (Phen), Erbium oxide (Er₂O₃) and dibenzoylmethane (DBM) were purchased from J&K, Da Mao Reagent (Tianjin, China), Jin Cheng Yuan Co., Ltd (Ganzhou,

China) and Aldrich (USA) separately. Methacrylic acid (HMA), glycidyl methacrylate (GMA) and other reagents were purchased from SCR (Shanghai, China) and Aladdin. They were used without further purification. 2, 2'-Azobisisobutyronitrile (AIBN), recrystallized freshly, was used as free-radical initiator. Copolymers were obtained by free-radical polymerization of dilute monomer solutions. All of the solvents were used after purification according to conventional methods.

2.2 Synthesis of Er Chloride Hexahydrate (ErCl₃·6H₂O)

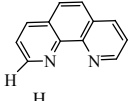
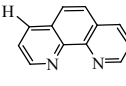
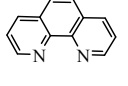
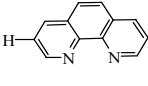
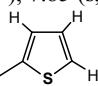
A total of 0.01 mol (3.825 g) of Er₂O₃ was dissolved in 40 mL of hydrochloric acid (HCl, 35 wt.%) under stirring at 100 °C. The product (ErCl₃·6H₂O) was obtained after evaporating excess HCl, washing with deionized water, and drying in vacuum. Finally, the product was obtained as a pink crystal.

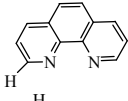
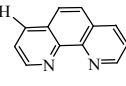
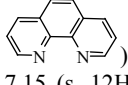
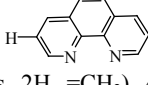
2.3 Synthesis of Er-Containing Organic Complexes (Er(TTA)₂(Phen)(MA), ErTPM)



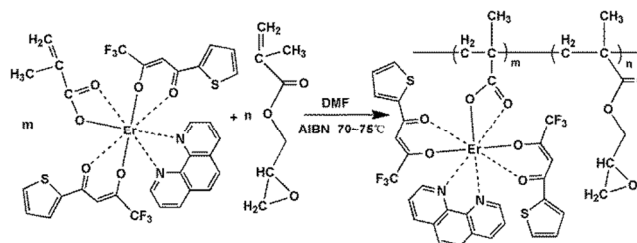
Scheme 1 Synthetic routes of complexes ErTPM and ErDPM

As shown in Scheme 1, TTA (0.889 g, 4 mmol) and Phen (0.396 g, 2 mmol) were dissolved in ethanol (30 ml, 95%) and then mixed with HMA liquid (0.207 g, 2.4 mmol) in a three-necked flask. The obtained solution was stirred and purged under N₂ at 50 °C. The pH value was carefully adjusted to 7.0–7.5 by adding 1 M NaOH in ethanol solution. After 30 min, 30 mL of 66.67 mM ErCl₃/ethanol solution was added slowly. With the addition of ErCl₃, the precipitate increased. The pH value of the mixed solution must be maintained between 7.0–7.5. The obtained solution was purged under N₂ for 20 h. The resulting complexes ErTPM were separated by using centrifugation and rinsed with ethanol several times. The product was dried under vacuum to reserve. The complexes Er(DBM)₂(Phen)(MA) (ErDPM) were then synthesized by using a similar method.

ErTPM ¹H NMR (400 MHz, DMSO, δ): 9.13 (s, 2H, , 8.58 (s, 2H, , 8.07 (s, 2H, , 7.85 (s, 2H, , 6.87 (s, 2H, =CH₂), 8.31 (s, 6H, , 3.40 (s, 3H, CH₃); IR (KBr, cm⁻¹): ν = 1630 (w, C=C), 1604 (vs, C=O), 1100-1300 (m, C-F).

ErDPM ¹H NMR (400MHz, CDCl₃, δ): 24.03 (s, 2H, , 22.61 (s, 2H, , 17.38 (s, 2H, , 9.59 (s, 2H, , 8.06 (s, 8H, -Ph), 7.15 (s, 12H, -Ph), 5.25 (s, 2H, =CH₂), 4.78 (s, 3H, CH₃); IR (KBr,cm⁻¹): 1620 (w, C=C), 1595 (vs, C=O).

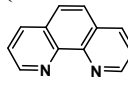
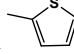
2.4 Free Radical Copolymerization of Poly (GMA-co-Er(TTA)₂(Phen)(MA)) (GETPM 2)



Scheme 2 Synthetic route of GETPM

As shown in Scheme 2, Er(TTA)₂(Phen)(MA) (0.096 g, 0.107 mmol), GMA (3.5 g, 25 mmol), and AIBN (0.015 g, 0.091 mmol) were dissolved in N,N-dimethylformamide (DMF, 40 mL) with stirring under a nitrogen atmosphere. The resulting solution was then heated at 70 °C for 6 h. The above-mentioned mixture was transferred to a 500 mL beaker containing 200 mL of methanol under stirring. The flocculent precipitate was separated by using centrifugation. The resulting polymer was dissolved in tetrahydrofuran (THF) and purified by precipitation in methanol; this procedure was repeated three times. The product (Er-containing 0.5%, GETPM 2) was then dried under vacuum. The yield of GETPM 2 was 90%. The molecular weight (Mn) was 38,000, and the polydispersity (PD) was 1.82.

Other Er-containing samples with different mass fractions of 0.3 wt. % (GETPM 1) and 1 wt. % (GETPM 3) were prepared by using a similar method and under the same experimental conditions.

(GETPM 2) ¹H NMR (400 MHz, DMSO-d₆, δ): 7.95 (m,  and , 4.30–3.74 (m, 2H, -CH₂-C-), 3.20 (m, H, -C-CH-), 2.80–2.66 (m, 2H, -C-CH₂-), 1.892 (d, 2H, -CH₂-), 0.98–0.81 (d, 3H, CH₃); IR (KBr,cm⁻¹): 1726 (vs, C=O), 907 (m, epoxy group).

Cite this: DOI: 10.1039/c0xx00000x

www.rsc.org/xxxxxx

ARTICLE TYPE

The other proportions of GETPM were synthesized by the same aforementioned method. All molar ratios of Er(TTA)₂(Phen)(MA) and GMA were 1:380 (GETPM 1, Er³⁺, 0.3 wt.%), 1:230 (GETPM 2, Er³⁺, 0.5 wt.%), and 1:115 (GETPM 3, Er³⁺, 1 wt.%).

2.5 Preparation of Crosslinked Polymer Films

To adhere well to the polymer, the Si wafer was first ultrasonically cleaned in organic solvents and immersed in an etchant consisting of H₂SO₄:H₂O₂=7:3 at 90 °C for 30 min. The Si wafer was rinsed with deionized water and dried by using nitrogen gas. Thin polymer films for the UV irradiation experiments were prepared by spin-coating on a Si wafer, with a N,N-dimethylformamide (DMF) solution containing 20–40 wt.% GETPM 2 and 1–2 wt.% PI. The UV irradiation was conducted with a 400 W UV lamp (365 nm) for at least 1 min. The resulting film, which was highly transparent, was baked in an oven at 120 °C for 1 h.

2.6 Measurements

IR spectra were taken on a Perkin-Elmer Spectrum 10 FT-IR infrared spectrophotometer. Nuclear magnetic resonance (NMR) spectra were measured on a Bruker ADVANCE NMR spectrometer at a resonance frequency of 400 MHz for ¹H NMR. The chemical shifts relative to TMS for ¹H NMR as internal reference are reported on the ppm scale. Average molar masses and molar mass distributions were determined by gel permeation chromatography (GPC) on a Waters 410 GPC with polystyrene as the standard and THF as the solvent. Differential scanning calorimetry (DSC) was performed with NETZSCH 4 at a scan rate of 10 °C/min under nitrogen. Thermal stability, as measured by 5% weight loss of the polymer samples, was analyzed using Perkin-Elmer TGA 7 analyzer at a heating rate of 10 °C/min in air. Atomic force microscopy (AFM) observations of the film surfaces were carried out with a commercial instrument (Digital Instrument, Nanoscope IIIa, Multimode) under ambient conditions at room temperature. All tapping mode images were measured at room temperature in air with the microfabricated rectangle crystal silicon cantilevers (Nanosensor). The UV-vis-NIR absorption spectra were recorded on SHIMADZU UV-3600 spectrophotometer (slit width 5 nm). UV-Vis photoluminescence (PL) spectra were conducted on a Perkin-Elmer LS55 luminescent spectrometer with a xenon lamp as a light source, the ex-slit width was 7.0 nm, and the em-slit width of the complexes and polymer were 7.0 nm respectively. In the measurements of infrared emission spectra, a continuous 480 nm wavelength was used to pump the samples. A visible photomultiplier (300–850 nm) and an infrared InAsGa detector (800–2200 nm) combined with a double-grating monochromator were used for spectral collection in the range of 400–2200 nm. Scanning electron microscopy (SEM) was performed on a JEOL JSM-6700F electron microscope with primary electron energy of 3 kV.

3. Result and Discussion

3.1 Luminescence Characterization of Er Complexes

For this study, the required Er complexes were synthesized by the reaction shown in Scheme 1. The resulting complexes, ErTPM and ErDPM, were characterized by UV-Vis-NIR absorption as powders. The UV-Vis-NIR absorption spectra of the Er complexes are illustrated in Fig. 1. The two complexes exhibit a series of absorption peaks in the region of 400–1600 nm and are mainly attributed to the energy levels that undergo reorganization, such as 492 nm (⁴I_{15/2} → ⁴F_{7/2}), 525 nm (⁴I_{15/2} → ²H_{11/2}), 550 nm (⁴I_{15/2} → ⁴S_{3/2}), 660 nm (⁴I_{15/2} → ⁴F_{9/2}), 800 nm (⁴I_{15/2} → ⁴I_{9/2}), 980 nm (⁴I_{15/2} → ⁴I_{11/2}), and 1530 nm (⁴I_{15/2} → ⁴I_{13/2}). The highest wavelength absorption peak (λ_{max}) for each complex reflects a transition from the lowest energy vibrational level in the ground state to the lowest energy vibrational level in the excited state (Fig. 2).

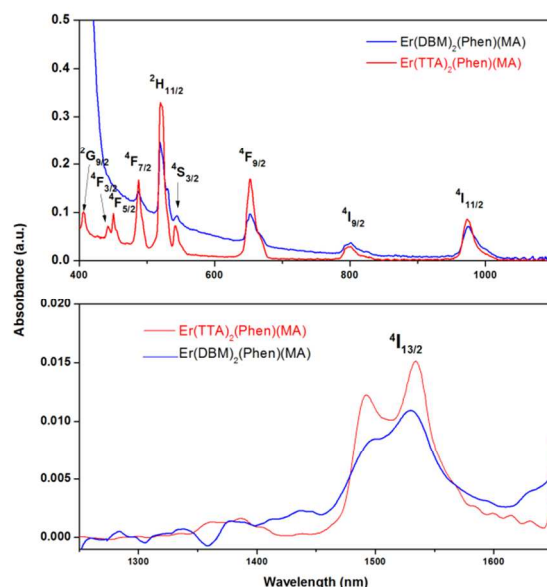


Fig. 1 The characteristic absorption spectra of organo-erbium complexes ErTPM and ErDPM in BaSO₄ tablets for UV-Vis, in KBr tablets for NIR. (all of the transitions shown are from the ⁴I_{15/2} ground state and labeled according to the excited state, using standard nomenclature).

The typical emission spectra of the two complexes were investigated as a KBr pellet (1 wt.%) at room temperature, and the characteristic emissions from the Er³⁺ excited state were observed (Fig. 3). The wavelengths of excitation were 390 nm.

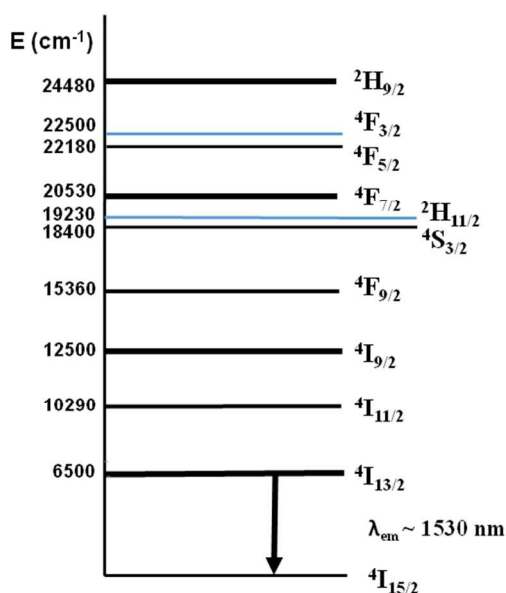


Fig. 2 Schematic excited states diagram for Er^{3+} in complexes in the range of 0-25000 cm^{-1} .

As shown in Fig. 3, the emission spectra exhibit characteristic emissions in the region of 430 – 600 nm after the transitions of $^4\text{F}_{5/2} \rightarrow ^4\text{I}_{15/2}$, $^4\text{F}_{7/2} \rightarrow ^4\text{I}_{15/2}$, and $^4\text{S}_{3/2} \rightarrow ^4\text{I}_{15/2}$ from the Er^{3+} .

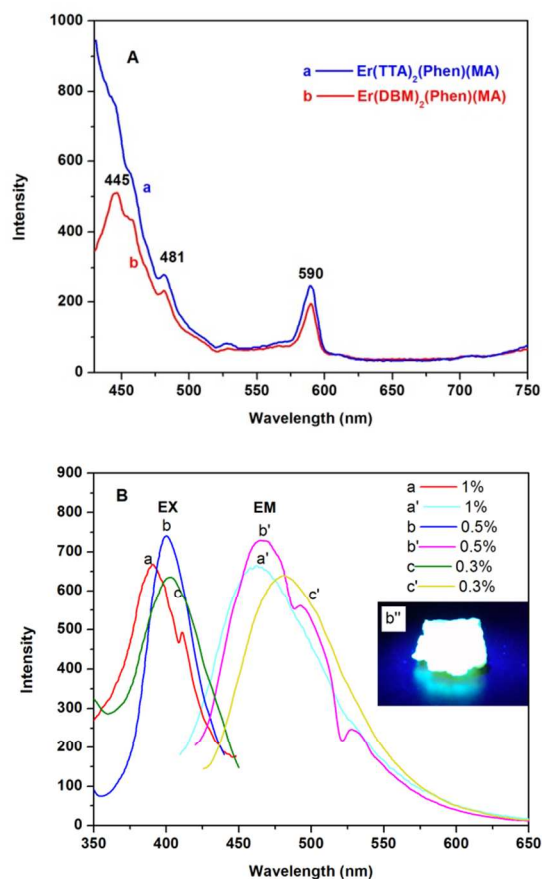


Fig. 3 Emission spectra for (A) complexes of $\text{Er}(\text{TTA})_2(\text{Phen})(\text{MA})$ (a, ErTPM) and $\text{Er}(\text{DBM})_2(\text{Phen})(\text{MA})$ (b, ErDPM) in KBr tablets (Er^{3+} : 1 wt.%) and (B) polymers of GETPM 3 (a', Er^{3+} : 1 wt. %), GETPM 2 (b', Er^{3+} : 0.5 wt.%) and GETPM 1 (c', Er^{3+} : 0.3 wt.%) in solid states were

excited at 390 nm. The excitation spectra for (B) polymers of GETPM 3 (a, Er^{3+} : 1 wt. %), GETPM 2 (b, Er^{3+} : 0.5 wt.%) and GETPM 1 (c, Er^{3+} : 0.3 wt.%). The luminescence photo of GETPM2 (b'') was excited at 375 nm.

The luminescence intensities resulting from the ErTPM (Fig. 3A. curve a) are obviously significantly higher than that from the ErDPM (Fig. 3A. curve b), thus indicating that the combined ErTPM ligands more effectively transfer the absorbed energy to the emitting level of the Er^{3+} . Therefore, we finally chose ErTPM as the monomer to synthesize the target product through free radical polymerization with GMA. As shown in Fig.3B, GETPM 2 (curve b') emits stronger characteristic luminescence than GETPM 3 (curve a'), and GETPM 1 (curve c') in solid states were excited at 390 nm.

3.2 Luminescence Characterization of Erbium Polymers

The NIR emission spectra of GETPMs with different proportions in the solid state were measured under the excitation of 480 nm. A dominant emission peak at around 1530 nm is characteristic of the electric dipole induced $^4\text{I}_{13/2} \rightarrow ^4\text{I}_{15/2}$ transition of the Er^{3+} . As shown in Fig. 4, the emission spectrum of ErTPM (curve a) exhibits almost identical characteristics: emission peak is broad (1500–1600 nm) and peak position is at 1530 nm for Er complexes^{25–28}. However, an interesting phenomenon occurred to the polymer (curves b, c, and d). The emission peaks of GETPMs obtained “narrow” emissions after the polymerization of ErTPM and GMA. This result has never been reported before perhaps because of the polymerization that restricts the transitions of Er^{3+} , which leave only a “single” $^4\text{I}_{13/2} \rightarrow ^4\text{I}_{15/2}$ level.

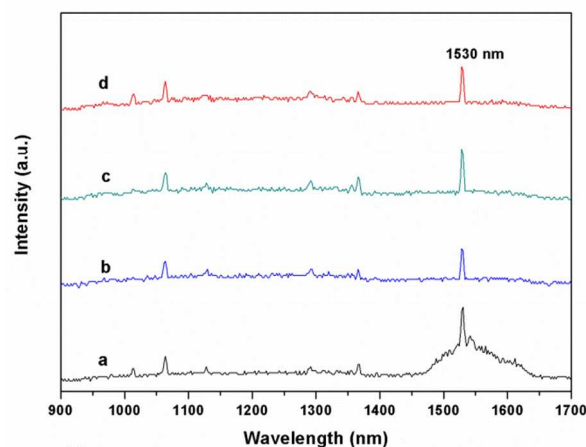


Fig 4. NIR photoluminescence spectra for complex of ErTPM in KBr tablets (a, 1 wt.%) and polymers of GETPM 1 (c, Er^{3+} : 0.3 wt. %), GETPM 2 (b, Er^{3+} : 0.5 wt. %) and GETPM 3 (d, Er^{3+} : 1 wt. %) in solid states, at a excitation wavelength of 480 nm ($75 \text{ mW}/\text{mm}^2$).

Moreover, the fluorescent intensity of GETPM 2 is higher than that of GETPM 1 and GETPM 3. At low concentrations, luminescence intensity increases with increasing Er^{3+} concentrations. Above the critical point, luminescence intensity will decrease because of luminescence-quenching occurring within the aggregates of Er^{3+} in GETPMs. We chose GETPM 2 (0.5 wt. % Er^{3+}) as the target product with the optimum proportion because of its aggregation and strong luminescence intensity.

Cite this: DOI: 10.1039/c0xx00000x

www.rsc.org/xxxxxx

ARTICLE TYPE

3.3 Properties of Thin Polymer Films

Atomic force microscopy (AFM) was used to study the morphology and surface uniformity of the cured GETPM 2 films. As shown in Fig. 5, the obtained AFM image indicates that the resulting films are fairly uniform and that no phase separation is observed. The root-mean-square surface roughness was 0.295 nm.

The cured polymers were found to have very good solvent resistance to common organic solvents such as N, N-dimethylformamide, chloroform, butyl acetate, and THF. Only less than 1% weight loss was observed after the resulting crosslinked polymer films were soaked in N, N-dimethylformamide for three days. These results indicate that the crosslinked polymer films possess good resistance to organic solvents.

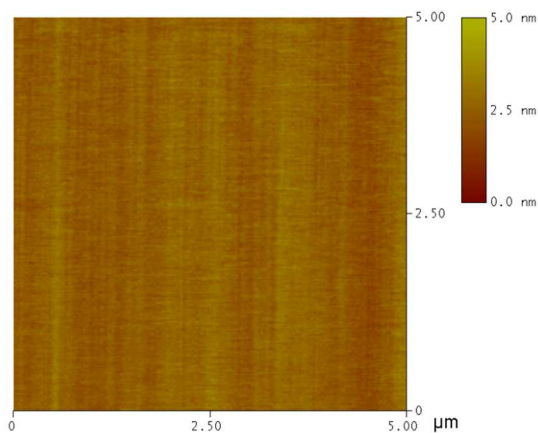


Fig. 5 Tapping mode AFM topograph of surface from the cured GETPM 2 films

3.4 Thermal Analysis

The thermal stabilities of GETPM 2 and that of the crosslinked polymer films were investigated by DSC and TGA measurements. As shown in Fig. 6, the glass transition temperature (T_g) of GETPM 2 (curve a) is approximately 142 °C, and the endothermic peak of crosslinked GETPM 2 (curve b) is not obvious because of the high crosslinking density. The TGA curves in Fig. 7 show that the decomposition temperatures (T_d , about 5%) of GETPM 2 is 265 °C and that the crosslinked GETPM 2 has good thermal stability with only 5% weight loss up to 303 °C. These parameters indicate that the 3D network of crosslinking forms a protective barrier against thermal decomposition while ensuring good thermal processability.

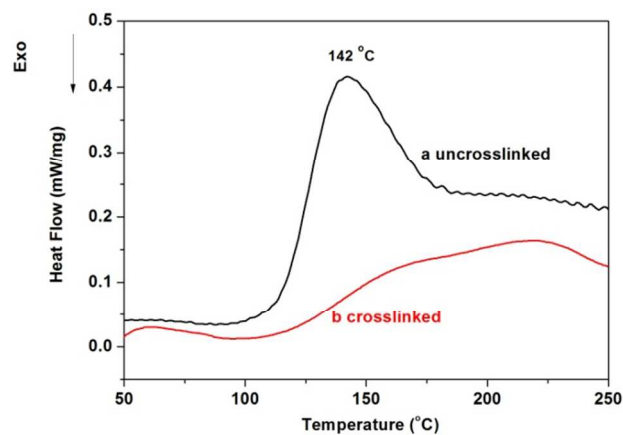


Fig. 6 DSC curves of GETPM 2 (a) and the crosslinked GETPM 2 (b)

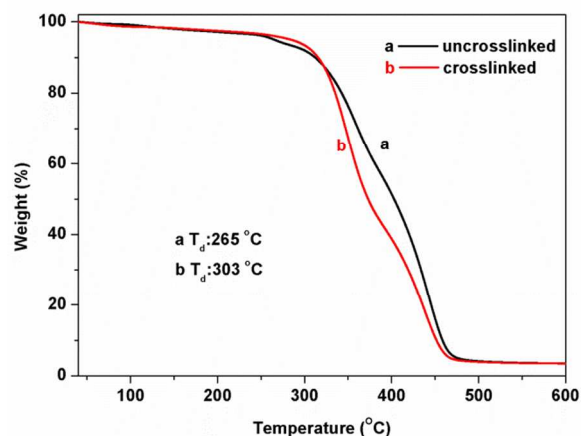


Fig. 7 TGA curves of GETPM 2 (a) and the crosslinked GETPM 2 (b)

3.6 Direct-Write UV lithography

Direct-write UV lithography is one of the most advantageous methods for fabricating micro patterns, even nanoscale structures, because of the small amount of steps involved^{29–35}. To fabricate different patterns, the GETPM solution containing a PI (2 wt. %) was first pin-coated onto the Si substrate to form polymer layers with 6–8 μm thicknesses. Thereafter, the baking process was performed (90 °C, 1 h) to remove solvents and a collimated UV beam was used to illuminate a contact mask on the films with a suitable exposure time (approximately 2 min). Finally, the films were baked (120 °C, 1 h) for the cationic polymerization of the epoxy group and then developed in DMF (5 min) to obtain the resulting micro patterns. The residual solvents were also removed by baking at 90 °C for 1 h. Fig. 8 shows the SEM image of the strip structure and indicates that the micro pattern has a smooth top surface and that the GETPM can be flexibly processed.

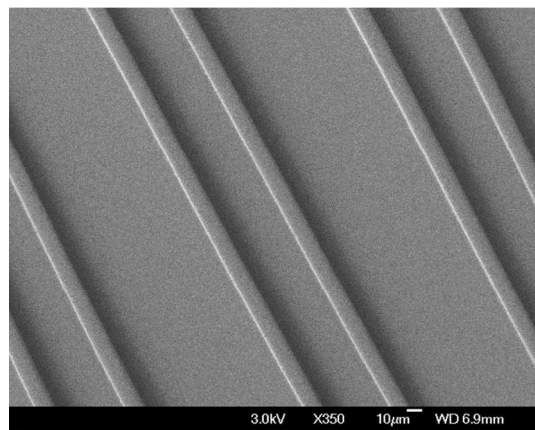


Fig. 8 SEM photograph of micro patterns fabricated with GETPM2

4. Conclusions

A novel Er-containing polymer was successfully synthesized by radical polymerization. The obtained Poly (GMA-co-Er(TTA)₂(Phen)(MA)) displays high green light and pure monochromatic NIR light (1530 nm). The good film-forming property and UV-light lithograph sensitivity of the novel Er-containing polymer make it easy to be processed. The crosslinked polymer film possesses good chemical resistance and high glass transition temperature and can be used in a variety of conditions. Micro patterns were fabricated from the Er-containing polymer by mask and direct UV exposure. The fabricated micro patterns exhibit smooth top surfaces. All excellent comprehensive properties make the polymer applicable in many fields, such as NIR-emitting devices, organic light emitting diodes, and fluorescent tags.

ACKNOWLEDGMENT

This work was supported by National Natural Science Foundation of China (No.21204007), Excellent talents support program of colleges and universities of liaoning province (LJQ2014054), Natural Science Foundation of Liaoning Province of China (2013020167), Open Project of State Key Laboratory for Supramolecular Structure and Materials (SKLSSM201425).

Notes and references

1 Instrumental Analysis Center, Dalian Polytechnic University, Dalian 116034, P. R. China

2 School of Textile and Material Engineering, Dalian Polytechnic University, Dalian 116034, P. R. China

3 School of Biological Engineering, Dalian Polytechnic University, Dalian 116034, P. R. China

† Electronic Supplementary Information (ESI) available: See DOI:10.1039/b000000x/

1. H. Q. Ye, Z. Li, Y. Peng, C. C. Wang, T. Y. Li, Y. X. Zheng, A. Sapelkin, G. Adamopoulos, I. Hernández, P. B. Wyatt, W. P. Gillin, *Nat. Mater.*, 2014, **13**, 382.
 2. H. Ma, A. K.-Y. Jen, L. R. Dalton, *Adv. Mater.*, 2002, **14**, 1339.
 3. A. Mech, A. Monguzzi, F. Meinardi, J. Mezyk, G. Macchi, R. Tubino, *J. Am. Chem. Soc.*, 2010, **132**, 4574.
 4. G. Mancino, A. J. Ferguson, A. Beeby, N. J. Long, and T. S. Jones. *J. Am. Chem. Soc.*, 2005, **127**, 524.

5. H.-Q. Ye, Y. Peng, Z. Li, C.-C. Wang, Y.-X. Zheng, M. Motevalli, P. B. Wyatt, W. P. Gillin, I. Hernández. *J. Phys. Chem. C*, 2013, **117**, 23970.
 6. C. Chen, D. Zhang, T. Li, D. M. Zhang, L. M. Song, Z. Zhen. *Appl. Phys. Lett.*, 2009, **94**, 041119.
 7. B. Y. Ahn, S. I. Seok, S. I. Hong, J.-S. Oh, H.-K. Jung, W. J. Chung. *Opt. Mater.*, 2006, **28**, 374.
 8. S. V. Eliseeva, J.-C. G. Bünzli, *Chem. Soc. Rev.*, 2010, **39**, 189.
 9. J.-C. G. Bünzli, C. Piguet, *Chem. Soc. Rev.*, 2005, **34**, 1048.
 10. K. Kuriki, Y. Koike, Y. Okamoto, *Chem. Rev.* 2002, **102**, 2347.
 11. J. S. Wang, J. Hu, D. H. Tang, X. H. Liu, Z. Zhen. *J. Mater. Chem.*, 2007, **17**, 1597.
 12. K. Yamashita, H. Taniguchi, S. Yuyama, K. Oe, J. Sun, H. Mataka. *Appl. Phys. Lett.*, 2007, **91**, 081115.
 13. J. Yang, M. B. J. Diemeer, D. Geskus, G. Sengo, M. Pollnau, A. Driessen. *Opt. Lett.*, 2009, **34**, 473.
 14. W. H. Wong, E. Y. B. Pun, K. S. Chan, *Appl. Phys. Lett.*, 2004, **84**, 176.
 15. A. Q. Le Quang, R. Hierle, J. Zyss, I. Ledoux. *Appl. Phys. Lett.*, 2006, **89**, 141124.
 16. S. Moynihan, R. Van Deun, K. Binnemans, G. Redmond. *Opt. Mater.*, 2007, **29**, 1821.
 17. S. Bo, J. Hu, H. X. Liu, Z. Zhen. *Opt. Comm.*, 2009, **282**, 2465.
 18. Y.X. Zheng, Y.H. Zhou, G. Accorsi, N. Armadori, *J. Rare Earths*, 2008, **26**, 173.
 19. M. C. Gather, A. Köhnen, A. Falcou, H. Becker, K. Meerholz, *Adv. Funct. Mater.*, 2007, **17**, 191.
 20. D. Losic, J. G. Mitchell, R. Lal, N. H. Voelcker, *Adv. Funct. Mater.*, 2007, **17**, 2439.
 21. X. Cheng, L. J. Guo, P. -F. Fu, *Adv. Mater.*, 2005, **17**, 1419.
 22. C. -W. Peng, K.-C. Chang, C. -J. Weng, M. -C. Lai, C. -H. Hsu, S. -C. Hsu, S. -Y. Li, Y. Wei, J. -M. Yeh, *Polym. Chem.*, 2013, **4**, 926.
 23. D. M. O'Carroll, C. E. Petoukho, J. Kohl, B. Yu, C. M. Carter, S. Goodman, *Polym. Chem.*, 2013, **4**, 5181.
 24. T. Griesser, A. Wolfberger, U. Daschiel, V. Schmidt, A. Fian, A. Jerrar, C. Teichert W. Kern, *Polym. Chem.*, 2013, **4**, 1708.
 25. Y. X. Zheng, M. J. Motevalli, R. H.C. Tan, I. Abrahams, W. P. Gillin, P. B. Wyatt. *Polyhedron*, 2008, **27**, 1503.
 26. A. Monguzzi, A. Milani, A. Mech, L. Brambilla, R. Tubino, C. Castellano, F. Demartin, F. Meinardi, C. Castiglioni, *Synthetic Metals*, 2012, **161**, 2693.
 27. I. Hernández, R. H. C. Tan, J. M. Pearson, P. B. Wyatt, W. P. Gillin, *J. Phy. Chem. B*, 2009, **113**, 7474.
 28. R. J. Curry, W. P. Gillin, A. P. Knights, R. Gwilliam, *Appl. Phys. Lett.*, 2000, **77**, 2271.
 29. S. Chatani, C. J. Kloxin, C. N. Bowman, *Polym. Chem.*, 2014, **5**, 2187.
 30. Y. Wan, X. Fei, Z. S. Shi, J. Hu, X. L. Zhang, L. S. Zhao, C. M. Chen, Z. C. Cui, D. M. Zhang, *J. Polym. Sci. Part A: Polym. Chem.*, 2011, **49**, 762.
 31. S. Q. Fan, X. Fei, X. Y. Wang, J. Tian, L. Q. Xu, P. Yang, Y. Wang, *React. Funct. Polym.*, 2014, **76**, 19.
 32. L. Li, K. W. Chen, L.C. Sun, S. Y. Xie, S. L. Lin, *React. Funct. Polym.*, 2013, **73**, 83.
 33. S. H. Kang, V. M. Prabhu, B. D. Vogt, E. K. Lin, W. L. Wu, K. Turnquest, *Polymer*, 2006, **47**, 6293.
 34. M. Yan, M. N. Wybourne, J. F. W. Keana, *React. Funct. Polym.*, 2000, **43**, 221.
 35. Z. F. Zhou, Q. A. Huang, W. H. Li, M. Feng, W. Lu, Z. Zhu, *J. Micromech. Microeng.*, 2007, **17**, 2538.